THE JOURNAL OF BIOLOGICAL CHEMISTRY
Vol. 276, No. 15, Issue of April 13, pp. 12153–12161, 2001

Printed in U.S.A.

The Crystal Structure of Human Placenta Growth Factor-1 (PlGF-1), an Angiogenic Protein, at 2.0 Å Resolution*

Received for publication, September 4, 2000, and in revised form, November 6, 2000
Published, JBC Papers in Press, November 7, 2000, DOI 10.1074/jbc.M008055200

Shalini Iyer‡§¶, Demetres D. Leonidas‡§‖, G. Jawahar Swaminathan‡, Domenico Maglione, Mauro Battisti**, Marina Tucci**, M. Graziella Persico‡‡§§ and K. Ravi Acharya‡¶¶**

*From the ‡Department of Biology and Biochemistry, University of Bath, Claverton Down, Bath BA2 7AY, United Kingdom, **Geymonat S.p.A., via S. Anna 2, 03012 Anagni (FR), Italy, and the ‡‡International Institute of Genetics and Biophysics, CNR, Via G. Marconi, 12-80125, Naples, Italy*

The angiogenic molecule placenta growth factor (PlGF) is a member of the cysteine-knot family of growth factors. In this study, a mature isoform of the human PlGF protein, PlGF-1, was crystallized as a homodimer in the crystallographic asymmetric unit, and its crystal structure was elucidated at 2.0 Å resolution. The overall structure of PlGF-1 is similar to that of vascular endothelial growth factor (VEGF) with which it shares 42% amino acid sequence identity. Based on structural and biochemical data, we have mapped several important residues on the PlGF-1 molecule that are involved in recognition of the fms-like tyrosine kinase receptor (Flt-1, also known as VEGFR-1). We propose a model for the association of PlGF-1 and Flt-1 domain 2 with precise shape complementarity, consider the relevance of this assembly for PlGF-1 signal transduction, and provide a structural basis for altered specificity of this molecule.

Angiogenesis, the process of new blood vessel formation, is essential for development, reproduction, wound healing, tissue regeneration, and remodeling (1). It also plays a major role in tumor progression, diabetic retinopathy, psoriasis, and rheumatoid arthritis (2). Angiogenesis involves proliferation of endothelial cells (ECs)[1] in an organized fashion and is most likely regulated by polypeptide growth factors (3, 4) such as acidic and basic fibroblast growth factors (aFGF and bFGF, Ref. 5), vascular endothelial growth factor (VEGF, Refs. 6–10), and placenta growth factor (PlGF, Refs. 11–14). PlGF, VEGF (VEGF-A), VEGF-B (15), VEGF-C (16), VEGF-D (17), VEGF-E (18), and Fos-induced growth factor (FIGF, Ref. 19) are members of a family of structurally related growth factors. Intra- and interchain disulfide bonds among eight characteristically spaced cysteine residues are involved in the formation of these active dimeric proteins and hence termed as cysteine-knot proteins. They also share a number of biochemical and functional features (for a review, see Ref. 20) such that PlGF and VEGF can form heterodimeric molecules in cells in which both genes are expressed (21, 22).

Alternative splicing of the PlGF primary transcript leads to three forms of the mature human PlGF protein (22–24). The two predominant forms, PlGF-1 and PlGF-2 (also known as PlGF-131 and PlGF-152, respectively), differ only by the insertion of a highly basic 21-amino acid stretch at the carboxyl end of the protein. This additional basic region confers upon PlGF-2 the ability to bind to heparin (13, 23).

The exact role of PlGF in vascular development is yet to be established. However, purification of PlGF-1 from overexpressing eukaryotic cells and measurement of angiogenic activity of the purified PlGF-1 *in vivo* in the rabbit cornea and chick chorioallantoic membrane (CAM) assays showed induction of a strong neovascularization process that was blocked by affinity-purified anti-PlGF-1 antibody. In the avascular cornea, PlGF-1 induced angiogenesis in a dose-dependent manner and seemed to be at least as effective (if not more effective) as VEGF and bFGF under the same conditions and at the same concentration. PlGF-1 was shown to induce cell growth and migration of endothelial cells from bovine coronary postcapillary venules and from human umbilical veins (HUVECs). In these two *in vitro* assays, PlGF-1 seemed to have a comparable effect on the cultured microvascular endothelium (*e.g.* capillary venule endothelial cells, CVECs) to that of VEGF and bFGF. These results clearly demonstrate that PlGF-1 can induce angiogenesis *in vivo* and stimulate the migration and proliferation of endothelial cells *in vitro* (25). In the case of PlGF-2 it has been established that the recombinant, purified protein is able to stimulate bovine aortic endothelial cells (BAEC, Ref. 13) and HUVECs but not the ECs from hepatic sinusoids (26).

The VEGF homodimer binds to and induces autophosphorylation of two distinct kinase receptors: the fms-like tyrosine kinase, Flt-1 (also known as VEGFR-1) and the kinase insert domain-containing receptor/fetal liver kinase, KDR/Flk-1 (also known as VEGFR-2). Conversely, the PlGF-1 and -2 homodimer bind only to the Flt-1 receptor (22, 26–28). Likewise, VEGF-B also binds selectively to Flt-1 and hence appears to be

* This work was supported by Medical Research Council (UK) Programme Grant 9540039 and Wellcome Trust (UK) Equipment Grant 055505/98/Z (to K. R. A.). The costs of publication of this article were defrayed in part by the payment of page charges. This article must therefore be hereby marked "*advertisement*" in accordance with 18 U.S.C. Section 1734 solely to indicate this fact.

The atomic coordinates and structure factors (code 1FZV) have been deposited in the Protein Data Bank, Research Collaboratory for Structural Bioinformatics, Rutgers University, New Brunswick, NJ (http://www.rcsb.org/).

§ These authors contributed equally to this work.

¶ Postgraduate training bursary from the University of Bath, United Kingdom.

‖ Present address: Inst. of Biological Research and Biotechnology, The National Hellenic Research Foundation, 48 Vas Constantinou Ave., Athens 11635, Greece.

§§ Recipient of the Associazione Italiana Ricerca sul Cancro (Italy) Research Grant.

¶¶ To whom correspondence should be addressed. Tel.: 44-1225-826238; Fax: 44-1225-826779; E-mail: K.R.Acharya@bath.ac.uk.

[1] The abbreviations used are: ECs, endothelial cells; PlGF, placenta growth factor; VEGF, vascular endothelial growth factor; FIGF, Fos-induced growth factor; PDGF-BB, platelet-derived growth factor-BB; TGF-β2, transforming growth factor-β2; NGF, nerve growth factor; Flt-1, fms-like tyrosine kinase; KDR/Flk-1, kinase insert domain-containing receptor/fetal liver kinase; VEGFR, VEGF receptor; HUVECs, human umbilical veins endothelial cells; MPD, 2-methyl-2,4-pentanediol; r.m.s., root mean square.

TABLE I
Crystallographic statistics

Dataset	PlGF-1
Data collection statistics	
Unit cell dimensions ($P4_3$, 1 homodimer/a.u.)	a = b = 62.6 Å, c = 84.1 Å
Resolution (Å)	40–2.0
Reflections measured	161,044
Unique reflections	21,067
R_{sym} (%)[a]	6.3
I/σI (outermost shell)	19.6 (3.6)
Completeness (outermost shell) (%)	99.4 (98.8)
Refinement statistics	
R_{cryst} (%)[b]	21.6
R_{free} (%)[c]	24.7
Number of protein atoms (homodimer)	1,546
Number of solvent molecules (homodimer)	132
R.m.s. deviation in bond lengths (Å)	0.010
R.m.s. deviation in bond angles (°)	1.5
Average B-factor for protein atoms (Å^2)	32.6
Average B-factor for main-chain atoms (Å^2)	32.6
Average B-factor for side-chain atoms (Å^2)	32.7
Average B-factor for solvent molecules (Å^2)	44.8
B-factor (from Wilson plot) (Å^2)	33.9

[a] $R_{sym} = \Sigma(|I_j - \langle I\rangle|)/\Sigma\langle I\rangle$ where I_j is the observed intensity of reflection j, and $\langle I\rangle$ is the average intensity of multiple observations.
[b] $R_{cryst} = \Sigma||F_o| - |F_c||/\Sigma|F_o|$, where F_o and F_c are the observed and calculated structure factor amplitudes, respectively.
[c] R_{free} is equal to R_{cryst} for a randomly selected 4% subset of reflections not used in the refinement.

a closer homolog of PlGF in its receptor-binding profile (29). Purified heterodimeric VEGF/PlGF has been shown also to bind KDR/Flk-1 (22). The extracellular portion of both receptors consists of seven immunoglobulin (IgG)-like domains, and the receptors share 44% amino acid sequence homology. The IgG-like domain 2 of the Flt-1 receptor is responsible for the binding specificity of PlGF-1 and -2 (30–32). Furthermore, it has been reported that only PlGF-2 can recognize neuropilins-1 and -2, receptor molecules found at the endothelial surface, in a heparin-dependent fashion (33, 34).

Since PlGF has been shown to bind and induce autophosphorylation of Flt-1 but not KDR/Flk-1, it appears that PlGF should exert its mitogenic and chemotactic effects on ECs through the activation of the Flt-1 intracellular signaling pathway. PlGF induces DNA synthesis but not migration of porcine aortic ECs (PAE) overexpressing Flt-1 (28). However, recent findings that PlGF is mitogenic and chemotactic for CVECs and HUVECs *in vitro* (25) (discussed above), raise the question of whether PlGF induces Flt-1 directly to transduce mitogenic and chemotactic signals inside the cell or whether PlGF acts indirectly through a mechanism of decoy, as previously proposed by Park *et al.* (14).

The recent observation that Flt-1 is able to mediate signaling in HUVECs in response to both PlGF and VEGF, leading to distinct biological responses, suggests that Flt-1 does not act as

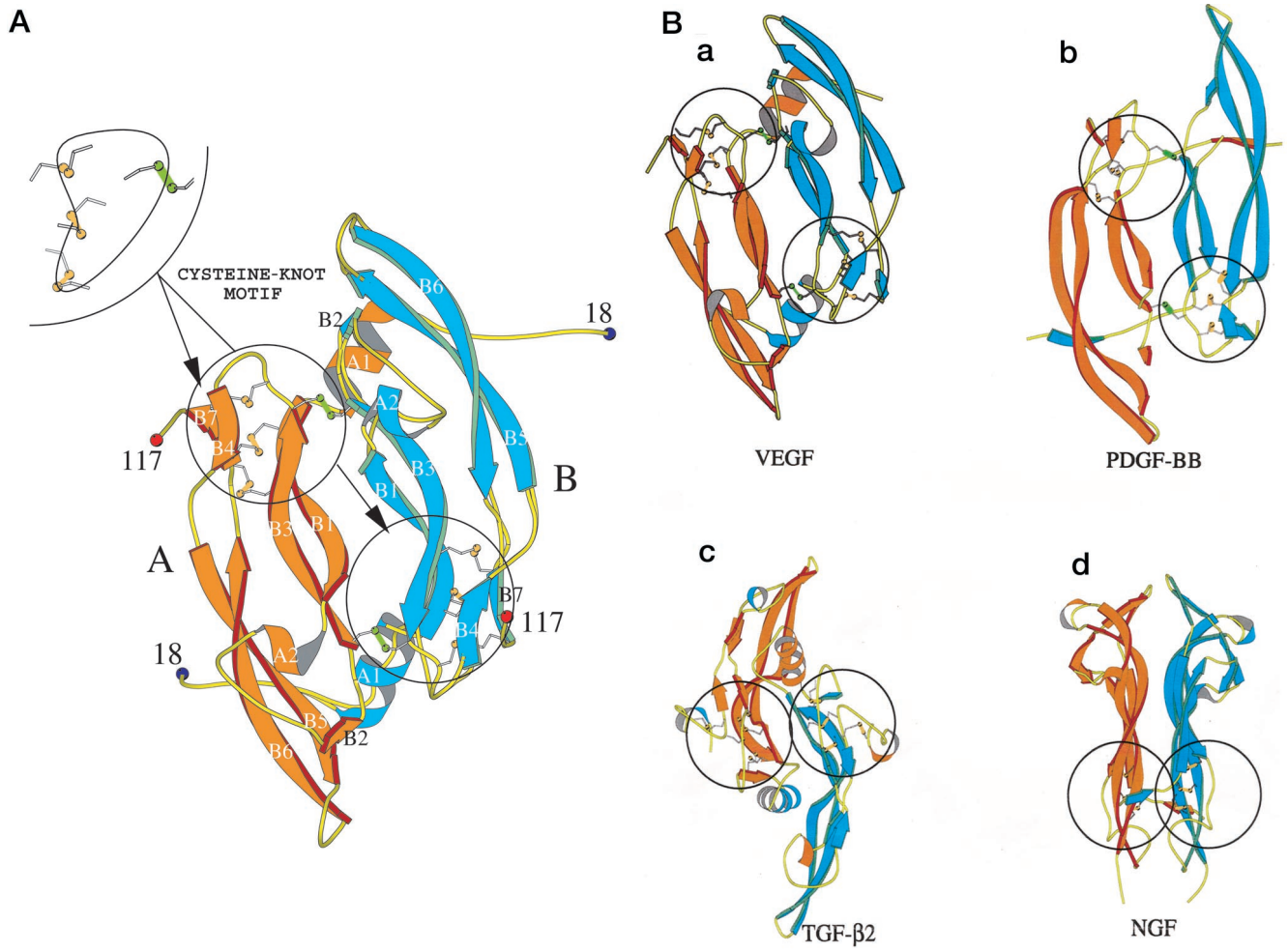

FIG. 1. **Structural comparison of PlGF-1 and other members of the cysteine-knot super family.** *A,* representation of the PlGF-1 homodimer structure. Disulfide bonds are shown in a *ball-and-stick* representation. The *inset* presents the organization of three intra- (in *yellow*) and one interdisulfide bridge (in *green*) in the cysteine-knot motif. Each monomer in the homodimer is colored differently to enhance clarity. *Orange*, monomer A; *cyan*, monomer B. *B,* representatives of known structures from the cysteine-knot protein family of dimeric molecules. *a,* VEGF (PDB code 2VPF, Ref. 39); *b,* PDGF-BB (PDB code 1PDG, Ref. 51); *c,* TGF-β2 (PDB code 1TFG, Ref. 52); and *d,* NGF (PDB code 1BTG, Ref. 53). With the exception of NGF, the homodimer 2-fold axis is perpendicular to the plane of the β-sheet. The cysteine knots are *highlighted*. *C,*

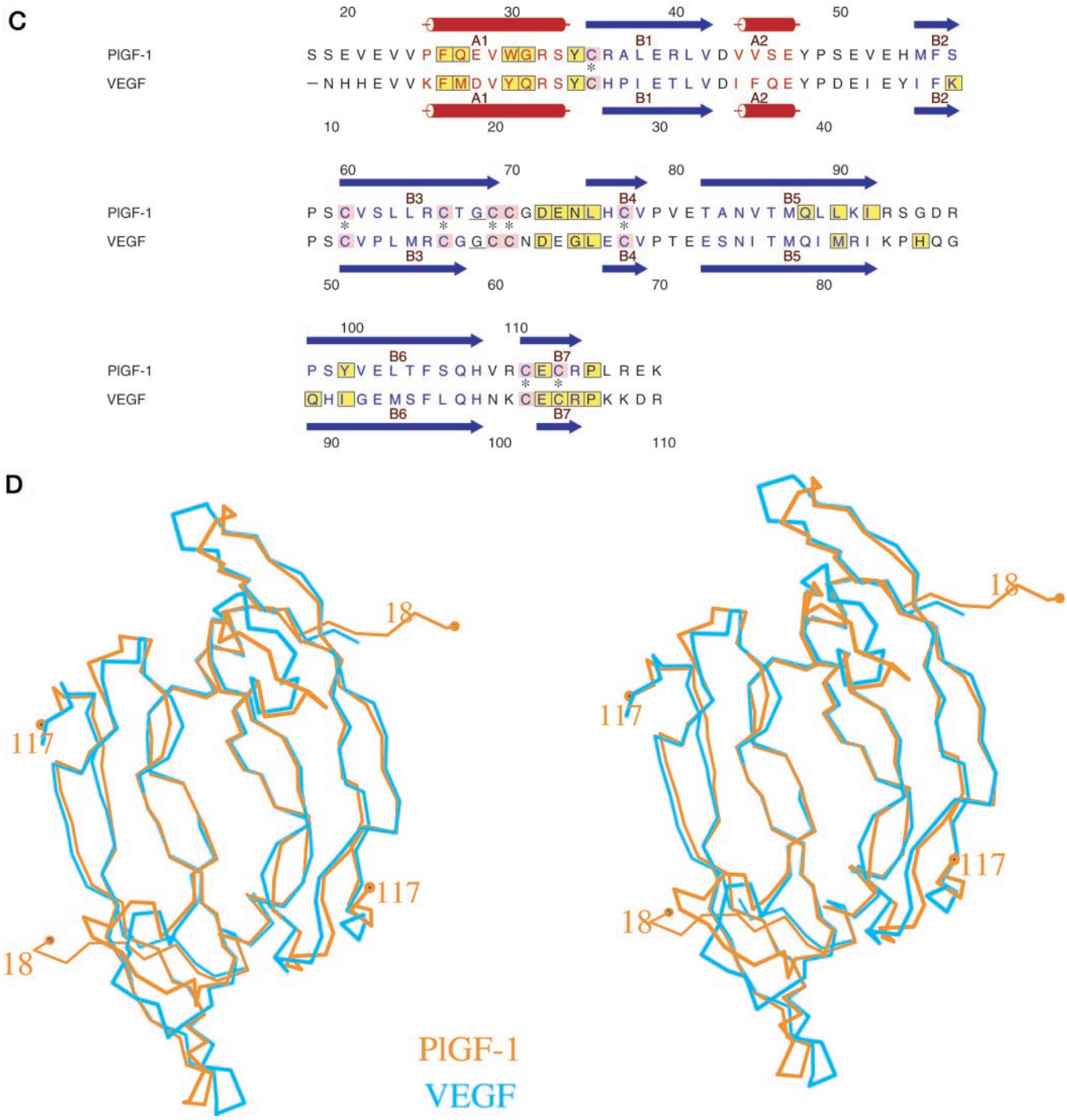

FIG. 1—*continued*

a decoy receptor but is indeed able to signal intracellularly (35). Inhibition of PlGF translation by antisense mRNA in the human dermal microvascular endothelial cells in culture results in the inhibition of cell proliferation under hypoxic conditions (36). These new findings assign a role to PlGF in the direct control of endothelial cell proliferation, probably competing with VEGF for binding to Flt-1 and thereby forcing the binding of VEGF to the KDR/Flk-1 and activating cell proliferation. In addition, both PlGF and VEGF are able to induce migration of 39% and 51% of monocytes, respectively, through activation of Flt-1 (35, 39). This suggests that PlGF may induce EC migration and proliferation through activation of Flt-1, although the existence of a yet unknown PlGF receptor cannot be ruled out.

A considerable amount of structural information is now

structure-based sequence alignment of PlGF-1 with VEGF (38, 39). Amino acid residues that form part of the secondary structural elements (β-strands and helices) as determined by DSSP (60) are shown in *blue* and *red,* respectively. The cysteine residues are shaded *pink*. VEGF residues involved in Flt-1 (VEGFR-1) binding (40), and the equivalent residues in PlGF-1 (based on a modeling study) are *boxed* and shaded in *yellow*. The conserved glycine residue in both structures is *underlined*. This figure was created with the program ALSCRIPT (61). *D,* stereo view displaying the Cα traces of PlGF-1 (*orange*) and VEGF (*cyan*) (39) homodimers after alignment of the two structures with the program "O" (49). *A*, *B,* and *D* were created with the program MOLSCRIPT (59).

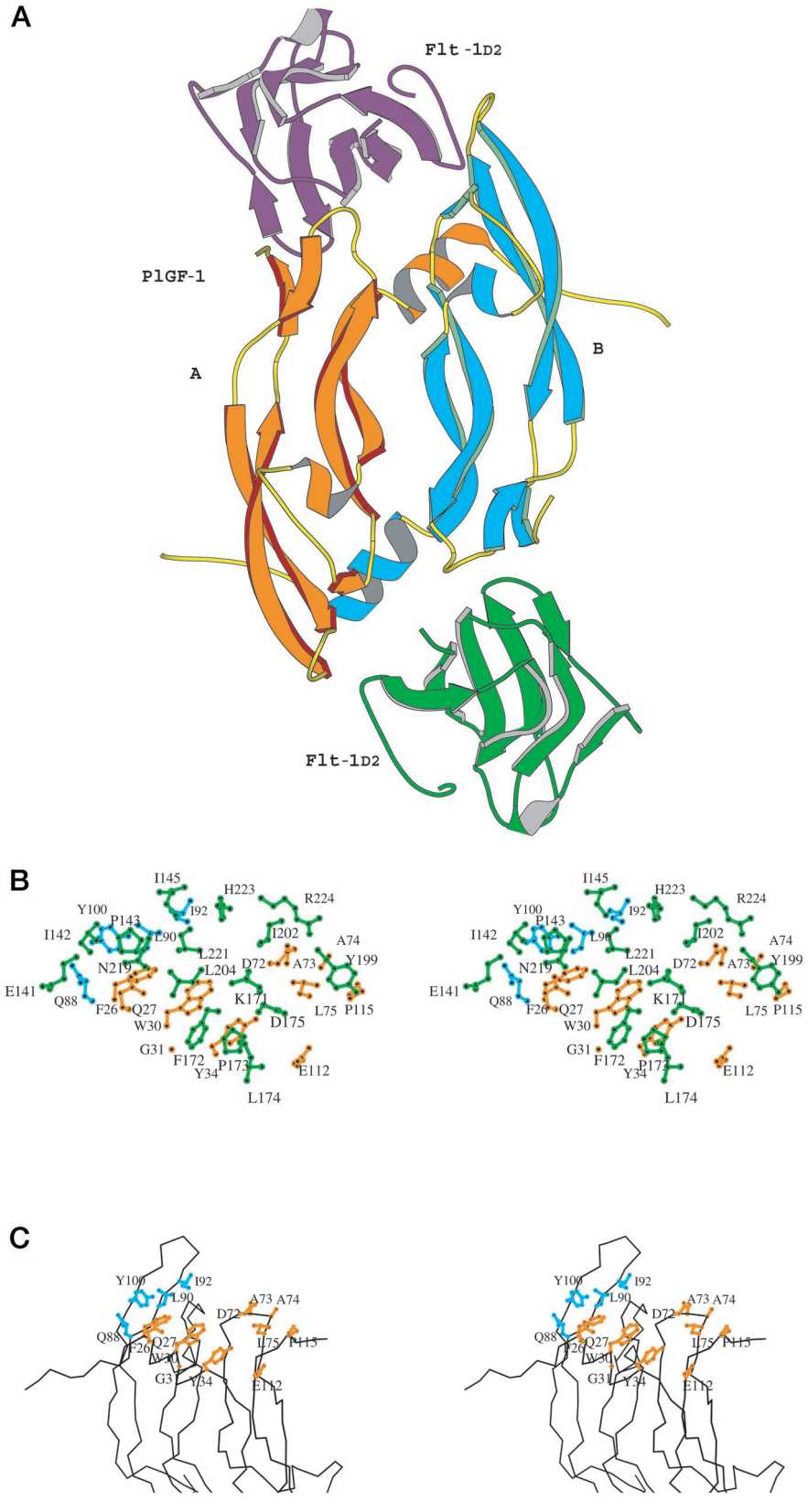

FIG. 2. **Proposed model for the PlGF-1·Flt-1_{D2} complex based on the crystal structures of PlGF-1 (present study) and the VEGF·Flt-1_{D2} complex (40), PDB accession code 1FLT.** *A,* PlGF-1 homodimer is shown in *orange* (molecule A) and *cyan* (molecule B), whereas the Flt-1_{D2} molecules are shown in *purple* and *green*. *B,* stereo views of contact residues (Cα atoms plus sidechain atoms) at the putative PlGF-1·Flt-1_{D2} interface. Residues from PlGF-1 monomers A and B are marked in *orange* and *cyan*, respectively. Residues from Flt-1 (figure based on model shown in *A*) are colored in *green*. The sidechains for Glu^{73} and Asn^{74} in free PlGF-1 are disordered and hence are treated as alanines. *C,* stereo views of contact residues (Cα atoms plus sidechain atoms) for PlGF-1. Residues from monomer A and B are marked in *orange* and *cyan,* respectively (figure based on model shown in *A*). The sidechains for Glu^{73} and Asn^{74} in free PlGF-1 are disordered and hence are treated as alanines. *D,* stereo views of contact residues (Cα atoms plus sidechain atoms) for Flt-1_{D2} (figure based on model shown in *A*). *E,* stereo views showing the location of the groove in PlGF-1 (residues Asp^{72}, Glu^{73}, Val^{52}, Met^{55}, Val^{45}, Asp^{43}, and Ser^{59}) and VEGF (Asp^{63}, Glu^{64}, Ile^{43}, Ile^{46}, Phe^{36}, Asp^{34}, and Ser^{50}), implicated for recognition of domain 3 of Flt-1 (40). The figure also shows the difference in conformation for segment 90–95 in PlGF-1 and 81–86 in VEGF. Residues Ile^{83}, Lys^{84}, and Pro^{85} are implicated in KDR recognition in VEGF (38), and the corresponding residues in PlGF-1 are Ile^{92}, Ser^{94}, and Arg^{93}. The sidechains for PlGF-1 and VEGF are shown in *orange* and *cyan,* respectively. Ser^{94} and Glu^{73} in the PlGF-1 structure are represented as alanines because of insufficient electron density beyond the Cβ atom. *A–E* was generated using MOLSCRIPT (59).

available for VEGF (VEGF-A). Muller *et al.* (38, 39) reported the crystal structures of the receptor binding domain of VEGF in different crystal forms and have identified the KDR binding site using mutational analysis. Also, Wiesmann *et al.* (40) have reported the crystal structure of VEGF in complex with domain 2 of Flt-1 (Flt-1_{D2}). To understand the specific molecular details of the receptor binding site and critical components of the homodimer, which will consequently help in understanding the differences in specificity and cross-reactivity among the VEGF homologs, we have embarked on a three-dimensional structural study of PlGF. Here we report the crystal structure of PlGF-1 at 2.0 Å resolution. As anticipated, the structure is

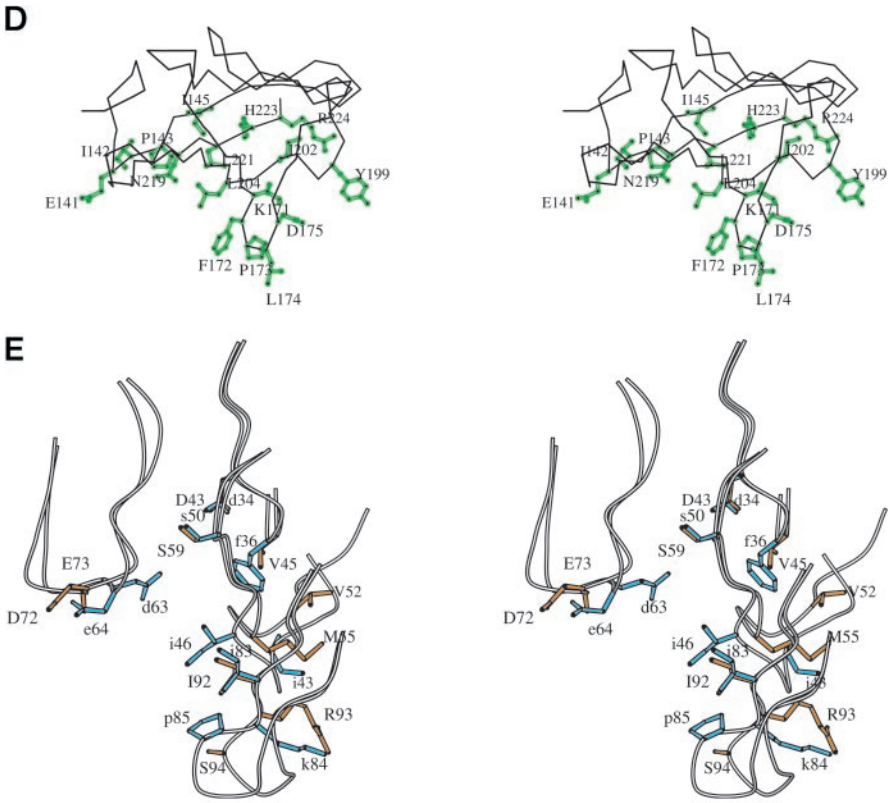

FIG. 2—*continued*

similar to that of VEGF. However, it shows subtle differences in molecular interactions at the receptor recognition site that appear to be relevant to signaling.

EXPERIMENTAL PROCEDURES

Protein Expression and Purification—By polymerase chain reaction, the region of the human *PlGF-1* gene coding for the mature protein was cloned into a prokaryotic expression vector as described previously (11). The recombinant vector was used to transform a DE3 *Escherichia coli* strain, and the synthesis of PlGF-1 was induced by 1 mM isopropyl-2-D-thiogalactopyranoside. After preparation and refolding of the inclusion bodies, the PlGF-1 protein was purified first by anion exchange chromatography followed by reverse phase chromatography. Final recovery of the active protein was about 140 mg per liter of initial bacterial culture. The identity of the protein was checked by various assays such as immunoblotting, SDS-polyacrylamide gel electrophoresis under reducing and nonreducing conditions, two-dimensional electrophoresis, reverse phase chromatography, and amino-terminal sequencing. The angiogenic activity was tested using a CAM assay (41); the purified bacterial-derived PlGF-1 was able to induce a strong and dose-dependent angiogenic response (42).

Crystallization—Crystals of recombinant PlGF-1 were grown using the hanging drop vapor diffusion method from drops containing 8 mg/ml protein at pH 6.0 in 0.05 M MES buffer, 10 mM $CaCl_2$ and 7.5% (v/v) 2-methyl-2,4-pentanediol (MPD) equilibrated against reservoirs containing 0.1 M MES buffer (pH 6.0), 20 mM $CaCl_2$ and 15% (v/v) MPD. Single crystals appeared after 5–6 days at 16 °C. These crystals could be flash-frozen at 100 K using a cryoprotectant solution containing 0.1 MES buffer (pH 6.0), and 30% (v/v) MPD. The systematic absences and symmetry were consistent with the tetragonal space group $P4_1$ or $P4_3$, with unit cell dimensions a = b = 62.6 Å, and c = 84.1 Å. There was one PlGF-1 homodimer per crystallographic asymmetric unit and ~50% of the crystal volume was occupied by solvent.

Data Processing and Reduction—X-ray diffraction data to 2.0 Å were collected at 100 K from a single crystal using the Synchrotron Radiation Source (station PX 9.5) at Daresbury (United Kingdom). Seventy images were collected (λ = 1.0 Å, oscillation range of 1.5°, 45 s exposure time) using a MAR-CCD detector system. Data processing was performed with the HKL package (43). Data reduction was carried out using the program TRUNCATE of the CCP4 suite (44). Details of data processing statistics are presented in Table I.

Phasing—The structure of PlGF-1 was determined by molecular replacement with the program AMoRe (45) using a polyalanine (homodimer) model based on the structure of VEGF at 1.93 Å resolution (PDB code 2VPF, Ref. 39). Data in the range 15.0–3.0 Å were used for both the rotation and the translation function searches. No solution was found in space group $P4_1$. In space group $P4_3$, the best solution after FITING had a correlation coefficient of 56% and an *R*-factor of 51%. Rigid-body refinement with CNS version 0.9 (46) of this model corresponding to the highest peak using data in the range 40.0–2.0 Å, resulted in an R_{free} and R_{cryst} of 44.6 and 40.6%, respectively.

Refinement—All crystallographic refinement was carried out using the program CNS version 0.9 (46). Procedures carried out with CNS included simulated annealing using a maximum likelihood target function, restrained individual B-factor refinement, conjugate gradient minimization, and bulk solvent correction. The behavior of the R_{free} value (811 reflections) was monitored throughout refinement. Several rounds of refinement (using all reflections) and model building were performed until the R_{free} for the model could not be improved any further. During the final stages of refinement, water molecules were inserted into the model at positions where peaks in the $|F_o|-|F_c|$ electron density maps had heights greater than 3σ and were at hydrogen bond forming distances from appropriate atoms. 2 $||F_o|-|F_c||$ ϕ_{calc} maps were also used to verify the consistency in peaks. Water molecules with a temperature factor greater than 65 $Å^2$ were excluded from the model and subsequent refinement. One bound MPD molecule per monomer from the crystallization medium was identified (interacting with the main-chain carbonyl oxygen atom of Thr-104 at one end and a water molecule at the other end) and was included in the final stages of the refinement. The details of refinement are presented in Table I. Map calculations were performed with CNS with the SigmaA protocol (47), using all the reflections in the resolution range 40.0–2.0 Å. The program PROCHECK (48) was used to assess the quality of the final structure. Analysis of the Ramachandran (φ-ψ) plot showed that all residues lie in the allowed regions. The program "O" (49) was used for map visualization and model building.

Accession Number—Final atomic coordinates of human PlGF-1 have been deposited with the RCSB Protein Data Bank under the accession code 1FZV.

TABLE II
Hydrogen bond interactions between the two monomers at the dimer interface in the PlGF-1 structure

Molecule A	Molecule B	Distance (Å)
Val^{24}–N	Thr^{86}–O	2.89
Val^{24}–O	Gln^{88}–N	2.89
Phe^{26}–N	Gln^{88}–Oε1	3.06
Arg^{32}–Nε	Glu^{39}–Oε1	2.79
Arg^{32}–Nη2	Glu^{39}–Oε2	3.22
Ser^{33}–Oγ	Cys^{60}–O	2.78
Arg^{36}–Nη2	Glu^{39}–Oε1	2.45
Glu^{39}–Oε1	Arg^{32}–Nε	3.02
Glu^{39}–Oε1	Arg^{36}–Nη1	2.77
Glu^{39}–Oε2	Arg^{36}–Nη2	3.26
Cys^{60}–O	Ser^{33}–Oγ	2.78
Thr^{86}–O	Val^{24}–N	2.89
Gln^{88}–N	Val^{24}–O	2.88
Gln^{88}–Oε1	Phe^{26}–N	2.86

RESULTS AND DISCUSSION

Quality of the Structure—The crystal structure of PlGF-1 was determined at 2.0 Å resolution. Details of the data collection and refinement statistics are shown in Table I. The protein crystallizes as a homodimer in the asymmetric unit. As in the VEGF structure (38), the first 17 amino-terminal residues of both monomers are not visible in the electron density map and were excluded from crystallographic refinement. Both monomers A and B contain residues 18–117. Also, residues Ser^{18}, Glu^{51}, Glu^{73}, Asn^{74}, and Ser^{94} in both molecules and residues Glu^{53} and Arg^{117} in molecule A have been modeled as alanines because of lack of sufficient density beyond Cβ atoms. The arrangement of the homodimer and the nomenclature used throughout the text are shown in Fig. 1*A*. The final model (homodimer) includes 1,546 non-hydrogen protein atoms, 132 water molecules, and two MPD molecules with a crystallographic *R*-factor (R_{cryst}) of 21.6% in the resolution range 40.0–2.0 Å. The R_{free} value is 24.7% with 4% of the reflections excluded from the refinement (50). The mean coordinate error calculated from a plot of ln σ_A *versus* $(\sin\theta/\lambda)^2$ is 0.3 Å. The root mean square (r.m.s.) deviation in Cα atoms between each monomer of the pair is 0.43 Å (for 100 Cα atoms). Regions that deviate most include residues 18–19 from the amino-terminal tail, part of the loop connecting strands β3 and β4 (residues 72–73), and the carboxyl-terminal residue 117. Excluding these residues improves the r.m.s deviation to 0.17 Å (for 94 Cα atoms). Examination of the Ramachandran plot shows 91.5% of the residues in most favorable regions and no residues in disallowed regions.

Overall Structure—The crystal structure of PlGF-1 consists of a homodimer, organized in an antiparallel arrangement with the 2-fold axis perpendicular to the plane of the β-sheet (Fig. 1*A*). The homodimer is covalently linked by two interchain disulfide bonds between Cys^{60} and Cys^{69}. The most prominent feature of the structure is the presence of a cysteine-knot motif, positioned symmetrically opposite at one end of each monomer. This motif is found in other closely related growth factors such as VEGF (38, 39), platelet-derived growth factor-BB (PDGF-BB, Ref. 51), transforming growth factor-β2 (TGF-β2, Ref. 52) and nerve growth factor (NGF, Ref. 53) (Fig. 1*B*). The knot consists of an eight residue ring formed by one interchain (Cys^{60}–Cys^{69}) and three intrachain (Cys^{35}–Cys^{77}, Cys^{66}–Cys^{111}, Cys^{70}–Cys^{113}) disulfide bonds (Fig. 1*A*). The ring structure is formed between two adjacent β-strands, β3 and β7, with the third intrachain disulfide bond penetrating the covalent linkage and connecting strands β1 and β4. The cysteine ring contains a conserved glycine residue at position 68, which seems to be important in optimizing the conformation of the sidechains in the knot. As in the VEGF structure (38, 39), this residue adopts positive dihedral φ angles of 141 and 149° in monomers A and B, respectively. Thus the cysteine-knot motif appears to be important for the stabilization of the dimer as there are only a few contacts between the β-strands (β1 and β1′) at the dimer center. One peptide bond in the PlGF-1 structure adopts a *cis* conformation: that connecting Ser^{57} and Pro^{58} in both monomers.

The structural core of the PlGF-1 monomer consists of a four-stranded, highly irregular, solvent-accessible β-sheet (Fig. 1*A*). The total buried surface area at the interface between the two monomers is 2,627 $Å^2$. A considerable proportion of this (1,830 $Å^2$ or 69%) is accounted for by the extensive intermolecular hydrophobic core interactions at the interface on the opposite end of the cysteine-knot and provides additional stability to the central portion of the structure. The hydrophobic core is formed by residues from both monomers and is known to be part of the receptor binding region of PlGF-1 (see under "Receptor Recognition"). Fourteen potential hydrogen bond interactions were observed between the two monomers (Table II). Two water-mediated hydrogen bonds between Glu^{39} from each monomer forms a bridge between two strands (β1 and β1′) across the center of the dimer interface.

Comparison with VEGF Structure—Overall, the structure of PlGF-1 exhibits remarkable topological identity with that of VEGF (38, 39) (with which it has 42% amino acid sequence identity) despite significant functional diversity (Fig. 1, *B—D*, r.m.s deviation of 1.47 Å using 95 Cα atoms). The mode of dimerization for PlGF-1 is similar to that of VEGF. Conformational differences between PlGF-1 and VEGF are observed at the amino-terminal residues (18–25), some residues from loop regions (loops connecting β3–β4, β5–β6, and α2–β2) and the carboxyl-terminal residues (116–117). Interestingly, these loop regions appear to be part of the receptor-binding face in both molecules (see below). Approximately 70 water molecules are conserved in PlGF-1 and VEGF and appear to be important for the structural integrity of the homodimer in both molecules.

Receptor Recognition—The extracellular domain of both KDR and Flt-1 receptors consist of seven immunoglobulin domains. Mutational analysis of VEGF has revealed that symmetrical binding sites for KDR are located at each pole of the VEGF homodimer (38). Each site appears to contain two functional regions composed of binding determinants presented across the intermolecular interface. This experimental evidence suggested that only a small number of VEGF residues are important for binding to KDR, and the binding epitope for KDR contains two hot-spots, each of which extends across the dimer interface (39, 54–56). Furthermore, analysis of the conformational variability of VEGF (based on the high resolution structure of VEGF, Ref. 39) showed that the loop connecting strands β5 to β6 undergoes a concerted movement. This loop is important for binding to both Flt-1 and KDR, suggesting that these receptor molecules have overlapping binding sites on the target molecule. It has also been established that minimally domains 2 and 3 of Flt-1 are necessary and sufficient for binding VEGF with near native affinity, and domain 2 alone binds to VEGF (60-fold less tightly than wild-type, Ref. 38). Similar results have been found for deletions in the KDR (56).

Recently, the crystal structure of VEGF in complex with Flt-1_{D2} (at 1.7 Å) has revealed that domain 2 is predominantly involved in hydrophobic interactions with the poles of the VEGF dimer (40). Based on this structure and previous mutagenesis data, Wiesmann *et al.* (40) have proposed a model of VEGF bound to the first four domains of Flt-1. In the case of PlGF, it has been shown that binding of PlGF to human ECs revealed a high affinity site and a low affinity site (35, 37). The high affinity site is for Flt-1 and PlGF can displace VEGF from

TABLE III
Putative intermolecular contacts

Putative intermolecular contacts between PlGF-1 and Flt-1_{D2} at the receptor interface in the modeled complex (left) and intermolecular contacts between VEGF and Flt-1_{D2} at the receptor interface (right) as observed from the crystal structure of VEGF · Flt-1 complex (40).

PlGF-1	Flt-1_{D2} Polar (< 3.4 Å)	Distance	VEGF	Flt-1_{D2} Polar (< 3.4 Å)	Distance
		Å			Å
Molecule A			Molecule A		
Gln^{27}–Oε1	Asn^{219}–Nδ2	3.15	Asp^{63}–Oδ1	Arg^{224}–Nη2	2.54
Asp^{72}–Oδ1	Arg^{224}–Nε	3.33	Asp^{63}–Oδ2	Arg^{224}–Nε	2.85
Asp^{72}–Oδ1	Arg^{224}–Nη2	3.18	His^{86}–Nδ1	Gln^{225}–Nε2	2.84
Ala^{74}–N	Arg^{224}–Nη2	3.12	Gln^{89}–Nε2	His^{147}–Nε2	3.40
			Arg^{105}–Nη1	Tyr^{199}–OH	3.31
Molecule B			Molecule B		
Tyr^{34}–OH	Lys^{171}–Nζ	3.33	Tyr^{25}–OH	Lys^{171}–Nζ	3.35
Asp^{72}–Oδ1	Arg^{224}–Nε	3.04	Lys^{48}–Nζ	His^{223}–Nδ1	3.22
Tyr^{100}–OH	Pro^{143}–O	3.19	Arg^{105}–Nη1	Tyr^{199}–OH	3.23
Glu^{112}–Oε2	Asp^{175}–Oδ1	3.03	Arg^{105}–Nη2	Tyr^{199}–OH	3.00
			Asp^{63}–Oδ1	Arg^{224}–Nη2	2.74
			Asp^{63}–Oδ1	Arg^{224}–Nε	3.33
			Asp^{63}–Oδ2	Arg^{224}–Nε	2.68

PlGF-1	Flt-1_{D2} van der Waals contacts[a]	Contacts	VEGF	Flt-1_{D2} van der Waals contacts[a]	Contacts
		Å			Å
Mol A			Mol A		
Phe^{26}	Pro^{143}(2), Leu^{221}(2)[b]	4	Phe^{17}	Ile^{142}, Pro^{143}(3)	4
Gln^{27}	Pro^{143}(2), Leu^{204}(3), Asn^{219}(3)	8	Met^{18}	Glu^{141}, Leu^{204}	2
Trp^{30}	Leu^{221}	2	Tyr^{21}	Gly^{203}, Leu^{204}(6)	7
Tyr^{34}	Lys^{171}, Phe^{172}(4), Pro^{173}(2)	7	Gln^{22}	Phe^{172}	4
Asp^{72}	Tyr^{199}, Ile^{202}(8), Arg^{224}	10	Tyr^{25}	Lys^{171}, Phe^{172}, Pro^{173}(2)	4
Ala^{73c}	Arg^{224}	2	Lys^{48}	Leu^{221}, His^{223}	2
Ala^{74c}	Arg^{224}	3	Asp^{63}	Ile^{202}(2), Arg^{224}(8)	10
Leu^{75}	Tyr^{199}	5	Gly^{65}	Arg^{224}	1
Gln^{88}	Ile^{142}	1	Leu^{66}	Tyr^{199}	1
Leu^{90}	Ile^{145}	1	Met^{81}	Leu^{221}	1
Tyr^{100}	Ile^{142}	3	His^{86}	Gln^{225}	6
Glu^{112}	Leu^{174}	1	Gln^{89}	His^{147}	1
Pro^{115}	Tyr^{199}	12	Ile^{91}	Ile^{142}	2
			Cys^{104}	Tyr^{199}	2
			Pro^{106}	Tyr^{199}	7
Mol B			Mol B		
Phe^{26}	Pro^{143}(4), Leu^{221}(2)	6	Phe^{17}	Ile^{142}, Pro^{143}(2), Leu^{221}	4
Gln^{27}	Glu^{141}(3), Ile^{142}, Pro^{143}(9), Leu^{204}, Asn^{219}(3)	17	Met^{18}	Asn^{219}	1
Trp^{30}	Leu^{204}	1	Tyr^{21}	Gly^{203}(2), Leu^{204}(6), Leu^{221}	9
Gly^{31}	Phe^{172}	2	Gln^{22}	Phe^{172}	8
Tyr^{34}	Phe^{172}(10), Pro^{173}(2)	12	Tyr^{25}	Phe^{172}	1
Asp^{72}	Ile^{202}, Arg^{224}(9)	10	Asp^{63}	Arg^{224}	8
Asn^{74}	Arg^{224}	3	Gly^{65}	Arg^{224}	2
Leu^{75}	Tyr^{199}	3	Leu^{66}	Arg^{224}	2
Gln^{88}	Ile^{142}	2	Met^{81}	Pro^{143}	1
Leu^{90}	Ile^{145}	2	Gln^{89}	Ile^{145}, His^{147}	2
Ile^{92}	His^{223}	5	Ile^{91}	Ile^{142}	5
Tyr^{100}	Ile^{142}(10), Pro^{143}(2)	12	Glu^{103}	Lys^{200}	1
Glu^{112}	Asp^{175}	5	Cys^{104}	Tyr^{199}	2
Pro^{115}	Tyr^{199}	9	Arg^{105}	Tyr^{199}, Lys^{200}(2)	3
			Pro^{106}	Tyr^{199}	3

[a] van der Waals distances are the maximum allowed values of C–C, 4.1Å; C–N, 3.8Å; C–O, 3.7Å; O–O, 3.3Å; O–N, 3.4Å; and N–N, 3.4Å.
[b] Numbers in parentheses represent the number of contacts made with the indicated Flt-1 residue. Hydrogen bond parameters and van der Waals contacts were calculated with the program CONTACT (44).
[c] Glu^{73} and Asn^{74} are modeled as alanines due to insufficient electron density for the sidechain atoms in the free PlGF-1 structure.

both truncated and full-length Flt-1 receptors. However, at the present time it is yet be established whether both PlGF-1 and VEGF bind identically to Flt-1.

Flt-1 (VEGFR-1) Receptor Interactions—The structure reported here for PlGF-1 is an unliganded structure and hence it is not possible to establish the precise nature of the interaction of PlGF-1 with Flt-1. However, using the structural data on the VEGF·Flt-1_{D2} complex, we have been able to construct a model to visualize the binding mode between PlGF-1 and Flt-1. The PlGF-1·Flt-1_{D2} complex was modeled by superimposing the atomic coordinates of the VEGF·Flt-1_{D2} complex (Ref. 40, PDB code 1FLT) onto the PlGF-1 model followed by energy minimization using the program X-PLOR (57). The resultant model showed a reasonable fit between PlGF-1 and Flt-1 without any obvious stereochemical impediments between the two proteins (Fig. 2*A*). The interface of the putative PlGF-1·Flt-1_{D2} complex appears to include some 22 amino acids from the PlGF-1 molecule: residues from the α1 helix, β3-β4 loop, and β7 strand of one monomer, and residues from strands β5, β6, and the β5-β6 loop of the second monomer. In the modeled complex, nineteen residues from the Flt-1_{D2} segments 141–147, 171–175, 199–204, and 219–226 form part of this contact surface. Modeling studies based on the VEGF·Flt-1_{D2} complex structure (40) predict that binding between PlGF-1 and Flt-1_{D2} might also be mediated through hydrophobic interactions involving planar surfaces from both the ligand and the receptor (Table III). Such

shape complementarity is energetically favorable for maximizing the contribution of van der Waals contacts.

Based on the PlGF-1·Flt-1_{D2} model, we speculate that both PlGF-1 and Flt-1_{D2} form extensive contacts through sidechain interactions (Table III, Fig. 2*B*). The contact residues from the two individual components of the modeled complex are shown in Fig. 2, *C* and *D*. Asp^{72} in PlGF-1 appears to be the only residue to make direct H-bond interactions with Arg^{224} of Flt-1_{D2}. (In the VEGF·Flt-1_{D2} complex structure, the conserved VEGF residue Asp^{63} makes similar interactions with Flt-1, Ref. 40, Table III.) PlGF-1 residues Gln^{27}, Tyr^{34}, Ala^{74}, Tyr^{100}, and Glu^{112} in one molecule (either A or B) are predicted to make both polar and van der Waals interactions with Flt-1, whereas residues Phe^{26}, Trp^{30}, Gly^{31}, Glu^{73}, Leu^{75}, Gln^{88}, Leu^{90}, Ile^{92}, and Pro^{115} seem to participate in van der Waals interactions with Flt-1 residues (Table III). Additional PlGF-1 residues Pro^{25}, Cys^{70}, Gly^{71}, Pro^{98}, Cys^{111}, Cys^{113}, and Arg^{114} also appear to be part of the interface.

A general mechanism of Flt-1 recognition by PlGF-1 can be postulated based on the proposed dimeric model of the receptor binding domain of VEGF in complex with domains 1–4 of Flt-1 (40). A similar picture may be visualized for PlGF-1·Flt-1 recognition with domain-1 pointing away from PlGF-1, the domain 2–3 linker region occupying the groove (6.8 Å wide) between the two monomers, and domain 3 making contact with its bottom face, which would bring domain 4 into direct inter-receptor contacts and hence involved in dimer formation. In the PlGF-1 structure, the walls of the groove are formed by residues Asp^{72}, Glu^{73}, Val^{52}, Met^{55}, Val^{45}, Asp^{43}, and Ser^{59}. The corresponding groove in VEGF was formed by residues Asp^{63}, Glu^{64}, Ile^{43}, Ile^{46}, Phe^{36}, Asp^{34}, and Ser^{50}, which was implicated for recognition of domain 3 of Flt-1 (40). This comparison illustrates a high degree of conservation of residues in this region between the two molecules (Fig. 1*C*). However, at the structural level, one can visualize significant changes in conformation (Fig. 2*E*), which could be one of the contributing factor for the distinct receptor specificity for PlGF-1 (see below).

Lack of KDR (VEGFR-2) Recognition—A detailed mutagenesis study of VEGF by Muller *et al.* (38) identified eight amino acid residues forming part of the KDR binding site. These were grouped as major and minor hot-spots for receptor recognition. The major hot-spot consists of two important residues Ile^{46} and Ile^{83} (VEGF numbering) and four additional residues Ile^{43}, Glu^{64}, Lys^{84}, and Pro^{85} with slightly lesser importance. The minor hot-spot contains residues Phe^{17} and Gln^{79} (38). Furthermore, recently a variant of VEGF, which had amino acids 83–89 replaced with the analogous region of the related PlGF demonstrated significantly reduced KDR binding compared with wild-type VEGF emphasizing the point that this region is important for VEGF-KDR interaction (58). Amino acid sequence alignment (Fig. 1*C*) shows that of the six most important KDR binding determinants (the major hot-spot) of VEGF, only two residues from VEGF (Glu^{64} and Ile^{83}) are conserved in PlGF-1 (Glu^{73} and Ile^{92}) and both residues from the minor hot-spot are conserved in the two structures. Observation of the PlGF-1 structure indicates significant conformational rearrangement corresponding to regions 43–45 and 83–85 (the major hot-spot residues for KDR recognition in VEGF, Fig. 2*E*). This provides a possible structural explanation for the inability of PlGF-1 to recognize KDR. Based on the amino acid sequence alignment of VEGF-A, PlGF-1, and VEGF-B, similar arguments can be put forward for VEGF-B, where considerable changes have appeared in the KDR binding determinants and hence may not recognize this receptor.

We have also performed modeling studies on the PlGF-1·VEGF heterodimer in complex with Flt-1_{D2} (in a similar way to that described above for the PlGF-1·Flt-1_{D2} complex). From this model, it appears that the putative contact residues in the heterodimer are similar to those listed in Table III for Flt-1 recognition.

Concluding Remarks—Recent structural studies on polypeptide growth factors in complex with their receptors have provided a wealth of information in the area of protein-receptor signaling. In the case of cysteine-knot proteins, the target molecule (*e.g.* VEGF, PDGF, or NGF) seems to form complexes with one or two domains of the receptor molecule. In this report, we have tried to address this question with another member of this family, PlGF-1, referring to the molecular details of a closely related molecule, VEGF. As in the case of VEGF, PlGF-1 appears to use only a small number of residues in receptor recognition. These details would be the starting point for the design of small mimics of PlGF. Such agonists could be useful for the design of PlGF antagonists, which prevent the interaction with the receptor, and may serve to be important for the treatment of pathological disorders involved in neovascularization during tumor growth.

Acknowledgments—We thank the staff at the Synchrotron radiation source, Daresbury (UK) for their help with X-ray data collection and members of the Acharya laboratory for constructive criticism of the manuscript.

REFERENCES

1. Folkman, J., and Shing, Y. (1992) *J. Biol. Chem.* **267,** 10931–10934
2. Folkman, J. (1995) *Nat. Med.* **1,** 27–31
3. Folkman, J., and Klagsbrun, M. (1987) *Science* **235,** 442–447
4. Risau, W. (1990) *Prog. Growth Factor Res.* **2,** 71–79
5. Klagsbrun, M. (1989) *Prog. Growth Factor Res.* **1,** 207–235
6. Ferrara, N., and Henzel, W. J. (1989) *Biochem. Biophys. Res. Commun.* **161,** 851–858
7. Keck, P. J., Hauser, S. D., Krivi, G., Sanzo, K., Warren, T., Feder, J., and Connolly, D. T. (1989) *Science* **246,** 1309–1312
8. Gospodarowicz, D., Abraham, J. A., and Schilling, J. (1989) *Proc. Natl. Acad. Sci. U. S. A.* **86,** 7311–7315
9. Levy, A. P., Tamargo, R., Brem, H., and Nathans, D. (1989) *Growth Factors* **2,** 9–19
10. Conn, G, Bayne, M. L, Soderman, D. D., Kwok, P. W., Sullivan, K. A., Palisi, T. M., Hope, D. A, and Thomas K. A. (1990) *Proc. Natl. Acad. Sci. U. S. A.* **87,** 2628–2632
11. Maglione, D., Guerriero, V., Viglietto, G., Delli-Bovi, P., and Persico, M. G. (1991) *Proc. Natl. Acad. Sci. U. S. A.* **88,** 9267–9271
12. Maglione, D., Guerriero, V., Viglietto, G., Risau, W., Delli-Bovi, P., and Persico, M. G. (1992) in *Growth factors of the vascular and nervous system* (Lenfant, C., Paoletti, R., and Albertini, A., eds), pp. 28–33, Karger, Basel
13. Hauser, S., and Weich, H. A. (1993) *Growth Factors* **9,** 259–268
14. Park, J. E., Chen, H. H., Winer, J., Houck, K. A., and Ferrara, N. (1994) *J. Biol. Chem.* **269,** 25646–25654
15. Olofsson, B., Pajusola, K., Kaipainen, A., von Euler, G., Joukov, V., Saksela, O., Orpana, A., Petersson, R. F., Alitalo, K., and Eriksson, U. (1996) *Proc. Natl. Acad. Sci. U. S. A.* **93,** 2576–2581
16. Joukov, V., Pajusola, K., Kaipainen, A., Chilov, D., Lahtinen, I., Kukk, E., Saksela, O., Kalkkinen, N., and Alitalo, K. (1996) *EMBO J.* **15,** 290–298
17. Achen, M. G., Jeltsch, M., Kukk, E., Makinen, M., Vitali, A., Wilks, A. F., Alitalo, K., and Stacker, S. A. (1998) *Proc. Natl. Acad. Sci. U. S. A.* **95,** 548–553
18. Meyer, M., Clauss M., Lepple-Wienhues, A., Waltenberger, J., Augustin, H. G., Zinche, M., Lanz, C., Buttner, M., Rziha, H-J., and Dehio, C. (1999) *EMBO J.* **18,** 363–374
19. Orlandini, M., Marconcini, L., Ferruzzi, R., and Oliviero, S. (1996) *Proc. Natl. Acad. Sci. U. S. A.* **93,** 11675–11680
20. Bussolino, F., Mantovani, A., and Persico, M. G. (1997) *Science* **22,** 251–256
21. Di Salvo, J., Bayne, M. L., Conn, G., Kwok, P. W., Trivedi, P. G., Soderman, D. D., Palisi, T. M., Sullivan, K. A., and Thomas, K. A. (1995) *J. Biol. Chem.* **270,** 7717–7723
22. Cao, Y. H., Chen, H., Zhou, L., Chiang, M. K., Anand-Apte, B., Weatherbee, J. A., Wang, Y. D., Fang, F. Y., Flanagan, J. G., and Tsang, M. L. S. (1996) *J. Biol. Chem.* **271,** 3154–3162
23. Maglione, D., Guerriero, V., Viglietto, G., Ferraro, M. G., Aprelikova, O., Alitalo, K., Del Vecchio, S., Lei, K. J., Chou, J. Y., and Persico, M. G. (1993) *Oncogene* **8,** 925–931
24. Cao, Y., Ji, W. R., Qi, P., Rosin, A., and Cao, Y. (1997) *Biochem. Biophys. Res. Commun.* **235,** 493–498
25. Ziche, M., Maglione, D., Ribatti, D., Morbidelli, L., Lago, C. T., Battisti, M., Paoletti, I., Barra, A., Tucci, M., Parise, G., Vincenti, V., Granger, H. J., Viglietto, G., and Persico, M. G. (1997) *Lab. Invest.* **76,** 517–531
26. Sawano, A., Takahashi, T., Yamaguchi, S., Aonuma, M., and Shibuya, M. (1996) *Cell Growth and Differ.* **7,** 213–221
27. Terman, B. I., Khandke, L., Dougher-Vermazan, M., Maglione, D., Lassam, N. J., Gospodarwicz, D., Persico, M. G., Bohlen, P., and Eisinger, M. (1994) *Growth Factors* **11,** 187–195

28. Landgren, E., Schiller, P., Cao, Y., and Claesson-Welsh, L. (1998) *Oncogene* **16,** 359–367
29. Olofsson, B., Korpelainen, E., Pepper, M. S., Mandriota, S. J., Aase, K., Kumar, V., Gunji, Y., Jeltsch, M. M., Shibuya, M., Alitalo, K., and Eriksson, U. (1998) *Proc. Natl. Acad. Sci. U. S. A.* **95,** 11709–11714
30. Davis-Smyth, T., Chen, H., Park, J., Presta, L. G., and Ferrara, N. (1996) *EMBO J.* **15,** 4919–4927
31. Barleon, B., Totzke, F., Herzog, C., Blanke, S., Kremmer, E., Siemeister, G., Marme, D., and Matiny-Baron, G. (1997) *J. Biol. Chem.* **272,** 10382–10388
32. Cunningham, S. A., Stephan, C. C., Arrate, M. P., Ayer, K. G., and Brock, T. A. (1997) *Biochem. Biophys. Res. Commun.* **231,** 596–599
33. Midgal, M., Huppertz, B., Tessler, S., Comforti, A., Shibuya, M., Reich, R., Baumann, H., and Neufeld, G. (1998) *J. Biol. Chem.* **273,** 22272–22278
34. Gluzman-Poltorak, Z., Cohen, T., Herzog, Y., and Neufeld, G. (2000) *J. Biol. Chem.* **275,** 18040–18045
35. Clauss, M., Weich, H., Breier, G., Knies, U., Rockl, W., Waltenberger, J., and Risau, W. (1996) *J. Biol. Chem.* **271,** 17629–17634
36. Yonekura, H., Sakurai, S., Liu, X., Migita, H., Wang, H., Yamagishi, S., Nomura, M., Abedin, M. J., Unoki, H., Yamamoto, Y., and Yamamoto, H. (1999) *J. Biol. Chem.* **274,** 35172–35178
37. Barleon, B., Sozzani, S., Zhou, D., Weich, H. A., Montovani, A., and Marme, D. (1996) *Blood* **87,** 3336–3343
38. Muller, Y. A., Li, B., Christinger, H. W., Wells, J. A., Cunningham, B. C., and de Vos, A. M. (1997) *Proc. Natl. Acad. Sci. U. S. A.* **94,** 7192–7197
39. Muller, Y. A., Christinger, H. W., Keyt, B. A., and de Vos, A. M. (1997) *Structure* **5,** 1325–1338
40. Wiesmann, C., Fuh, G., Christinger, H. W., Eigenbrot, C., Wells, J. A., and de Vos, A. M. (1997) *Cell* **91,** 695–704
41. Ribatti, D., Vacca, A., Roncali, L., and Dammacco, F. (1996) *Int. J. Dev. Biol.* **40,** 1189–1197
42. Maglione, D., Battisti, M., and Tucci, M. (2000) *Il. Farmaco* **55,** 165–167
43. Otwinowski, Z., and Minor, W. (1997) *Methods Enzymol.* **276,** 307–326
44. Collaborative Computational Project, Number 4 (1994) *Acta Crystallogr. Sect. D* **50,** 760–763
45. Navaza, J. (1994) *Acta Crystallogr. Sect. A* **50,** 157–163
46. Brünger, A. T., Adams, P. D., Clore, G. M., DeLano, W. L., Gros, P., Grosse-Kunstleve, R. W., Jiang, J. S., Kuszewski, J., Nilges, M., Pannu, N. S., Read, R. J., Rice, L. M., Simonson, T., and Warren, G. L. (1998) *Acta Crystallogr. Sect. D* **54,** 905–921
47. Read, R. J. (1986) *Acta Crystallogr. Sect. A* **42,** 140–149
48. Laskowski, R. A., MacArthur, M. W., Moss, D. S., and Thornton, J. M. (1993) *J. Appl. Crystallogr.* **26,** 283–291
49. Jones, T. A., Zou, J. Y., Cowan, S. W., and Kjeldgaard, M. (1991) *Acta Crystallogr. Sect. A* **47,** 110–119
50. Brünger, A. T. (1992a) *Nature* **355,** 472–475
51. Oefner, C., D'Arcy, A. D., Winkler, F. K., Eggimann, B., and Hosang, M. (1992) *EMBO J.* **11,** 3921–3926
52. Schlunegger, M. P., and Grutter, M. G. (1992) *Nature* **358,** 430–434
53. Holland, D. R., Cousens, L. S., Meng, W., and Matthews, B. W. (1994) *J. Mol. Biol.* **239,** 385–400
54. Keyt, B. A., Berleau, L. T., Nguyen, H. V., Chen, H., Heinsohn, H., Vandlen, R., and Ferrara, N. (1996) *J. Biol. Chem.* **271,** 7788–7795
55. Keyt, B. A., Nguyen, H. V., Berleau, L. T., Duarte, C. M., Park, J., Chen, H., and Ferrara, N. (1996) *J. Biol. Chem.* **271,** 5638–5646
56. Fuh, G, Li, B., Crowley, C, Cunningham, B., and Wells, J. A. (1998) *J. Biol. Chem.* **273,** 11197–11204
57. Brünger, A. T. (1992b) *X-PLOR Version 3.1 Manual: A System for X-ray Crystallography & NMR.* Yale University Press, New Haven
58. Stacker, S. A., Vitali, A., Caeser, C., Domagala, T., Groenen, L. C., Nice, E., Achen, M. G., and Wilks, A. F. (1999) *J. Biol. Chem.* **274,** 34884–34892
59. Kraulis, P. J. (1991) *J. Appl. Crystallogr.* **24,** 946–950
60. Kabsch, W., and Sanders, C. (1983) *Biopolymers* **22,** 2577–2637
61. Barton, G. J. (1993) *Protein Eng.* **6,** 37–40

The Crystal Structure of Human Placenta Growth Factor-1 (PlGF-1), an Angiogenic Protein, at 2.0 Å Resolution

Shalini Iyer, Demetres D. Leonidas, G. Jawahar Swaminathan, Domenico Maglione, Mauro Battisti, Marina Tucci, M. Graziella Persico and K. Ravi Acharya

J. Biol. Chem. 2001, 276:12153-12161.
doi: 10.1074/jbc.M008055200 originally published online November 7, 2000
